Available online at www.sciencedirect.com
ScienceDirect
Earth and Planetary Science Letters 263 (2007) 74–87
EPSL
www.elsevier.com/locate/epsl

Modelling shear bands in a volcanic conduit: Implications for over-pressures and extrusion-rates

Alina J. Hale *, Hans-B. Mühlhaus

Earth Systems Science Computational Centre (ESSCC), Australian Computational Earth Systems Simulator (ACcESS), The University of Queensland, Brisbane, QLD 4072, Australia

Received 20 December 2006; received in revised form 3 August 2007; accepted 28 August 2007
Available online 8 September 2007
Editor: C.P. Jaupart

Abstract

Shear bands in a volcanic conduit are modelled for crystal-rich magma flow using simplified conditions to capture the fundamental behaviour of a natural system. Our simulations begin with magma crystallinity in equilibrium with an applied pressure field and isothermal conditions. The viscosity of the magma is derived using existing empirical equations and is dependent upon temperature, water content and crystallinity. From these initial conduit conditions we utilize the Finite Element Method, using axi-symmetric coordinates, to simulate shear bands via shear localisation. We use the von Mises visco-plasticity model with constant magma shear strength for a first look into the effects of plasticity. The extent of shear bands in the conduit is explored with a numerical model parameterized with values appropriate for Soufrière Hills Volcano, Montserrat, although the model is generic in nature. Our model simulates shallow (up to approximately 700 m) shear bands that occur within the upper conduit and probably govern the lava extrusion style due to shear boundaries. We also model the change in the over-pressure field within the conduit for flow with and without shear bands. The pressure change can be as large as several MPa at shallow depths in the conduit, which generates a maximum change in the pressure gradient of 10's of kPa/m. The formation of shear bands could therefore provide an alternative or additional mechanism for the inflation/deflation of the volcano flanks as measured by tilt-metres. Shear bands are found to have a significant effect upon the magma ascent rate due to shear-induced flow reducing conduit friction and altering the over-pressure in the upper conduit. Since we do not model frictional controlled slip, only plastic flow, our model calculates the minimum change in extrusion rate due to shear bands. However, extrusion rates can almost double due to the formation of shear bands, which may help suppress volatile loss. Due to the paucity of data and large parameter space available for the magma shear strength our model results can only allow for a qualitative comparison to a natural system at this stage.
© 2007 Elsevier B.V. All rights reserved.

Keywords: magma flow; finite element method; shear bands; lava dome; computational volcanology; Soufrière Hills Volcano

1. Introduction

Lava domes form when the extruded lava is so viscous it cannot flow freely away from the vent. Such structures can grow slowly for many weeks to years without being a threat to the surrounding population, but occasionally, a lava dome may collapse or explode. The main risk from collapse events are pyroclastic flows, concentrated dispersions of hot volcanic fragments that move rapidly down the volcano flanks in response to gravity (Calder et al., 2002). Collapse events are a regular occurrence on Soufrière Hills Volcano (SHV),

* Corresponding author. Tel.: +61 7 3346 4110; fax: +61 7 3346 4134.
E-mail addresses: alinah@esscc.uq.edu.au (A.J. Hale), h.muhlhaus@uq.edu.au (H.-B. Mühlhaus).

0012-821X/$ - see front matter © 2007 Elsevier B.V. All rights reserved.
doi:10.1016/j.epsl.2007.08.026

Montserrat, and can take the form of repeated destruction and reconstruction of the dome, often with the locus of new growth switching over time.

Lava dome emplacement morphology ranges from near solid structures to more fluid flows, and is dominated by the degree of magma crystallisation (Watts et al., 2002; Sparks and Young, 2002). Crystal growth in intermediate composition magma occurs primarily due to the exsolution of volatiles, due to a decrease in pressure during ascent that acts to lower the liquidus temperature of the melt. Consequently, magma undergoes profound rheological stiffening during ascent, which can change the magma from a Newtonian fluid into a hot crystalline solid with only small amounts of residual melt (Sparks et al., 2000). Crystallisation is also time-dependent and for SHV, and lava domes generally, the morphology of the dome exhibits a high degree of correlation with the lava extrusion rate (Watts et al., 2002). At the lowest extrusion rates lava is highly crystalline (85 to 95% solid fraction) within the upper conduit. During these conditions lava dome growth occurs in a predominantly extrusive (exogenous) fashion, producing crystal-rich structures such as spines and whalebacks (Watts et al., 2002). At higher extrusion rates the magma has less time to crystallize in the conduit, resulting in more fluid-like behaviour including intrusive (endogenous) inflation and exogenous low aspect ratio flows.

During exogenous dome growth, lava is extruded directly to the free surface of the dome, implying some form of internal structure capable of channelling the magma. During emplacement the lava often extrudes in a stick-slip manner along curved structures, interpreted as ductile shear boundaries, suggesting that the conduit wall provides the main detachment surface. Spines, whalebacks and other crystal-rich exogenous structures commonly exhibit sub-parallel groves running along their length parallel with the direction of extrusion, that indicate some form of shear process (Sparks et al., 2000). Observational evidence of these structures also identifies cataclasites, suggesting the development of brittle shear bands (Tuffen et al., 2003). The lava extrusion style is therefore to some degree controlled by shear bands, their presence being fundamental in crystal-rich exogenous emplacement.

Three types of seismic signal are commonly observed during silicic volcanic eruptions: Volcano-Tectonic (VT) events thought to be indicative of rock fracture, Long-Period (LP) events characterized by their harmonic signature and interpreted as oscillations in a fluid-filled resonator, and Hybrids which have a high-frequency onset (VT) followed by a low-frequency ringing (LP) (Kumagai and Chouet, 1999; Neuberg et al., 2000). For SHV, the depth at which these seismic signals occur is anywhere between the free surface and 3000 m below it (Baptie et al., 2002). VT events represent the deeper conduit system and spikes in activity have generally been linked to significant changes in eruption activity, although they are more commonly recorded during periods of dormancy (Jaquet et al., 2006). Hybrid and LP events represent upper conduit and dome processes, commonly with the source location remaining relatively stable over-time (Jaquet et al., 2006). For SHV LP seismicity is calculated to originate approximately 1500 m below the surface of the dome (Neuberg et al., 2005).

Cyclic behaviour at SHV during 1997 was observed for seismicity, deformation of the volcano flanks as recorded by tilt-meters, as well as lava dome growth. During this period cycles ranged from 4–36 h (not including the Vulcanian explosion cyclic events) (Voight et al., 1999; Sparks and Young, 2002; Diller et al., 2006). During a typical (4–36 h) cyclic period on SHV, lava dome growth would stagnate, as measured by the seismic network signifying the accompanying rockfall activity from the dome was reduced (Calder et al., 2002). A reduction in the lava extrusion rate is indicative of crystal growth in the upper conduit, the timescales of which are comparable to the deformation cycles, leading to the formation of an impeding dense viscous plug (Diller et al., 2006). Pressurisation of magma and gas under the viscous plug can then result in the inflation of the volcano flanks. An acceleration in extrusion rate, observed by an increase in the amount of rockfalls from the advancing lava, signifies the formation of a new pathway for the lava and the removal of the viscous plug (Watts et al., 2002). This permits the pressure in the upper conduit to decrease, leading to the deflation of the volcano flanks. Typically dome growth is more pronounced at the peak of volcano flank tilt deformation and during deflation, commonly with extrusion rates approximately doubling and lava extrusion being accommodated by slip on ductile shear faults (Voight et al., 1999; Sparks and Young, 2002). The volcano flank deflations were generally more rapid than flank inflation, and hybrid earthquakes were observed to coincide with the point at which volcano flank inflation started to decelerate (the point of inflexion), suggesting that seismicity may be initiating the depressurisation process (Green and Neuberg, 2006).

The above evidence, along with additional observational data (Tuffen et al., 2003), has led some research groups to postulate that hybrid and LP seismic events originate from stick-slip processes along the conduit margin (Neuberg et al., 2005). Shear bands, as observed at the surface of the dome during cyclic activity, could generate such stick-slip behaviour, suggesting that shear bands could penetrate to the depths where LP seismicity

originates. Using an isotropically pressurised conduit model (Widiwijayanti et al., 2005), an elastic half-space model (Voight et al., 1999), or shear stresses at the wall of the conduit (Green et al., 2006), the depth of the pressure source is calculated to be less than 1000 m below the surface of the dome for SHV. Since the depth of LP events is approximately 1500 m below the surface of the dome, this means that the tilt and seismic hypocentres don't appear to correlate, however the calculated depths are strongly model dependent.

We develop a visco-plastic axi-symmetrical Finite Element Method (FEM) model to simulate the generation of shear bands, localised regions of high strain, in a conduit via shear-localisation. The formation of a zone or band of localised shear along the conduit wall occurs within our conduit domain when the material enters the plastic limit, i.e. when the shear stress experienced equals the shear strength of the magma. We neglect any potential frictional slip after shear bands have been generated, considering only plastic flow and therefore the minimum change in extrusion rate. We neglect the influence that bubbles have upon the viscosity and density, which may alter the flow properties. We also neglect departures from isothermal conditions and the evolution of shear bands once they form, instead considering the slow mode components of lava rheology, making the assumption that the timescales for shear band evolution occur more rapidly than the rheology can change. Instead, we focus our attention on a magma crystallinity in equilibrium with the pressure field and the influence this has upon viscosity and shear stress, which is found to be more significant than for bubbles for this style of volcanism (Bardintzeff and McBirney, 2000; Costa, 2005). For this paper we use constant magma shear strength because it is unknown which constitutive relationship controls the mode of deformation at depth. This means that the extent of the shear bands is controlled by the magma shear stress, which is effectively governed by the viscosity. Our model is intended to be simplified to capture the fundamental behaviour of a natural system, such as changes in extrusion rate and pressure. In Section 2 we briefly discuss existing models that consider shear bands in conduit flow. We follow this with the description of our conduit model in Section 3, including the field equations and initial conditions used. Section 4 provides results from our model and in Section 5 we discuss these results.

2. Existing models

Modelling efforts have been limited by the complexities of the magma rheology, for which no complete mathematical model currently exists (Hess and Dingwell, 1996). Costa (2005) recently developed an advanced model for the viscosity of magma containing very high solid fractions, although this model remains Newtonian. Existing numerical models have offered important insights into the fundamental characteristics of lava flow in a conduit due to gas exsolution and crystallisation and how this may promote cyclic behaviour. Hess and Dingwell (1996), Melnik and Sparks (1999, 2002, 2005) conduit models demonstrate that the major flow regimes depend upon the relative timescales of magma ascent and crystallisation, and that some cyclic behaviour can be attributed to the timescales involved with crystallisation kinetics. The observation of complex oscillatory behaviour in the high-pressure extrusion of industrial polymer melts led Denlinger and Hoblitt (1999) to develop a simple dynamic model for conduit flow. They model compressible magma flow though a cylindrical conduit undergoing stick-slip motion to extract characteristic oscillatory time-periods, and relate this to the cyclic periods experienced by silicic volcanoes. While Wylie et al. (1999) modelled volatile exsolution as magma nears the surface, the corresponding increase in magma viscosity within an elastic medium, and how this promotes oscillatory flow. In all these models the oscillatory and seismic behaviour is related to the magma flow instability. However, none of the models consider the lateral variations across the conduit which will modify the flow properties and promote the development of shear bands (Massol et al., 2001; Hale et al., in press).

Neuberg et al. (2005) combined seismological clues, field evidence and numerical modelling to suggest a trigger mechanism for LP seismicity based upon the brittle failure of magma in the glass transition. They model magma flow in a conduit using the FEM. Shear bands develop at the conduit wall where loss of heat and gas is modelled, consequently resulting in a high viscosity gradient. Although they base their model upon the SHV, they use a very low crystallinity of 30% and this means they have to rely upon very high extrusion rates to force the generation of shear bands to appropriate depths. Gonnermann and Manga (2003) use bubble growth and plastic failure to model the point at which magma fragmentation occurs within a conduit and the influence it has upon the resulting eruption style. For their model they are primarily interested in how magma melt and bubbles control viscous shearing, but do not specifically consider the depth that fragmentation (intense shear) occurs, or how it then changes the extrusion rate or pressure within the conduit. This is our motivation, and as for Neuberg et al. (2005) and Gonnermann and Manga (2003) we use an empirical well-studied viscosity and constant magma shear strength for a first look into the effects of plasticity.

3. Conduit model

We model the conduit as a vertical cylinder of uniform radius between the magma chamber and the volcano free surface, as shown in Fig. 1. The conduit is 15 m in radius and has a length of 5 km (Barclay et al., 1998). Magma ascent is driven by an over-pressure existing within the magma chamber, defined as the total pressure minus magma-static pressure, and the pressure at the free surface is atmospheric. Model equations are discussed in this section and Table 1 lists the parameters used in the model.

3.1. Momentum equations

Magma is modelled as an isotropic, incompressible viscous fluid. The relationship between the deviatoric part of the stress tensor σ'_{ij}, and the symmetric part of the velocity gradient or stretching D'_{ij}, reads:

$$\sigma'_{ij} = 2\eta D'_{ij}, i,j = (1,2,3), \tag{1}$$

where

$$\begin{aligned} \sigma'_{ij} &= \sigma_{ij} + P\delta_{ij} \quad \text{and} \quad P = -\frac{1}{3}\sigma_{kk}, \\ D'_{ij} &= D_{ij} - \frac{1}{3}D_{kk}\delta_{ij}. \end{aligned} \tag{2}$$

Here σ_{ij} are components of the stress tensor, η the viscosity, δ_{ij} is the Kronecker delta and P the pressure. In general the viscosity depends on the pressure, temperature and other state variables. Here we focus on the dependency of η on the crystal content as described in Sections 3.4 and 3.5. We also assume that any dilatancy effects associated with the crystallisation processes do not affect the qualitative features of the flows considered here; i.e. we assume:

$$D_{jj} = \mathrm{div}\mathbf{v} = 0, \tag{3}$$

where $\boldsymbol{v}$ is the velocity vector. The stress-equilibrium equations in axi-symmetrical coordinates, read,

$$\begin{aligned} &(r\sigma_{rr})_{,r} + r\sigma_{rz,z} - \sigma_{\theta\theta} + rf_r = 0 \\ &r\sigma_{zz,z} + (r\sigma_{rz})_{,r} + rf_z = 0. \end{aligned} \tag{4}$$

where f is the body force and r is the radial coordinate. Insertion of Eqs. (1) and (2) into 4 yields the equations of motion in the following form:

$$\begin{aligned} &\big(r\big(2\eta v_{r,r} - P\big)\big)_{,r} + r\big(\eta\big(v_{r,z} + v_{z,r}\big)\big)_{,z} - 2\eta\frac{v_r}{r} + P + rf_r = 0 \\ &r\big(2\eta v_{z,z} - P\big)_{,z} + \big(r\eta\big(v_{r,z} + v_{z,r}\big)\big)_{,r} + rf_z = 0. \end{aligned} \tag{5}$$

3.2. Generating shear bands

Shear bands are weak regions stressed under high strain-rates that are prone to failure. Localised shear bands form if the underlying flow or deformation experiences a particular type of instability in the constitutive relationship (Moresi et al., 2002). This instability expresses itself mathematically as a change in the type of the tangential boundary value problem. In pressure-sensitive materials the instability may arise because of a mismatch between the pressure sensitivity and the dilatancy factor and/or strain softening, for example due to micro-cracking. Another important shear band generating mechanism is related to shear heating and thermal feedback due to a strongly temperature-dependent viscosity. However, this mechanism is generally only relevant for high Péclet number flows (adiabatic shear banding) and is not likely to be important in our study due to the low flow rates experienced at SHV (Hale et al., in press). Model results are extremely mesh sensitive since the thickness of shear bands is undetermined in standard continuum models. Strategies to overcome this ill-posedness have been developed mainly by the engineering community (Mühlhaus and Vardoulkis, 1987). Here we accept this mesh sensitivity so that the shear band width will be set by the length scale provided by the discretisation scheme, i.e. the characteristic element width, which equals the thickness of shear bands observed at SHV (Sparks et al., 2000).

Magma flow rates can be highly variable due to complex feedback processes such as time-dependent crystallisation (Melnik and Sparks, 1999). However we need an initial crystallinity, pressure and viscosity within our conduit from which to initialise our model. The simplest starting point is to assume that the magma is initially stationary, and that the crystal content is in equilibrium with a pressure field. Stationary magma also implies that no shear bands currently exist within the conduit at the start of the simulation. From this initial magma state we need to initiate flow by changing the pressure field. Over timescales associated with magma ascent in the conduit, magma chamber key variables such as over-pressure are likely to be approximately constant due to its large volume with respect to the lava dome and conduit. Since our model is not transient at this stage we need to make the necessary simplification that a rapid over-pressure change occurs that is large enough to force magma flow and to generate shear bands. A significant and rapid pressure change within the conduit can be achieved by removing a flow-inhibiting lava dome, existing at the conduit exit, by means of a collapse event. Therefore our model begins with a pressure field that represents a lava

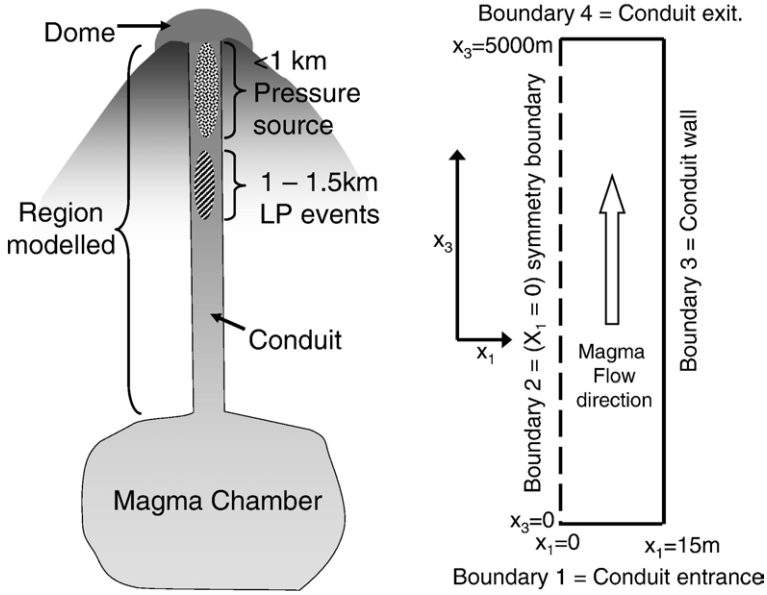

Fig. 1. Schematic of a volcano, showing a conduit connecting the magma chamber to the free surface, with lava dome/flow at the conduit exit (not to scale). In reality the conduit may narrow at depth but it is assumed to be a constant radius for simplicity in this model. Also shown is the approximate depth at which LP seismicity and pressurisation responsible for volcano flank tilt occurs. Shown next to the schematic is the model domain. We use axi-symmetric coordinates, modelling the conduit between $r=0$ to the conduit wall at $r=15$ m. The length of the conduit is 5000 m. Boundary 1 has the condition of an applied pressure, the magma chamber pressure, and Boundary 4 is at atmospheric pressure. Boundary 3 has the condition of no-slip and Boundary 2 is a symmetry boundary, ensuring no flow in the radial direction.

dome at the conduit exit, providing a resisting pressure equal to the magnitude of the over-pressure in the magma chamber. The initial pressure gradient from which to evaluate the magma properties in the conduit for one simulation thus comprises of a component from the magma-static pressure, plus a constant over-pressure from the weight of the lava dome. Mathematically we instantaneously remove the dome and set the conduit exit pressure to be equal to atmospheric pressure. The over-pressure existing within the magma chamber can then be transferred to the magma in the conduit enabling flow. The velocity and pressure fields within the conduit are then calculated iteratively, using the initialised viscosity field and conduit exit and magma chamber pressures as boundary conditions.

The largest dome recorded at SHV was approximately 1116 m above sea level, and following a collapse event the deepest it excavated into the crater was approximately

Table 1
Parameters used in the model which are appropriate for the magma from Soufrière Hills Volcano

Symbol	Parameter	Reference	Value
T	Initial temperature	Rutherford and Devine (2003)	1123°K
ϕ	Crystal volume fraction in chamber	Sparks et al. (2000)	0.6
ρ	Density	Melnik and Sparks (1999)	2350 kg m^{-3}
P_0	Maximum over-pressure	Sparks (1997)	20 MPa
ξ	Parameters in effective viscosity function	Melnik and Sparks (2005)	8.6
θ_0	Parameter in effective viscosity function	Melnik and Sparks (2005)	1.4
ϕ_0	Parameter in effective viscosity function	Melnik and Sparks (2005)	0.69
α_S	Solubility coefficient	Melnik and Sparks (1999)	4.11×10^{-6} Pa$^{-1/2}$
a_T	Liquidus and solidus coefficients	Melnik and Sparks (2005)	1465.4
b_T	Liquidus and solidus coefficients	Melnik and Sparks (2005)	−31.4
c_T	Liquidus and solidus coefficients	Melnik and Sparks (2005)	−2.8
d_T	Liquidus and solidus coefficients	Melnik and Sparks (2005)	−0.41
R_C	Conduit radius	Barclay et al. (1998)	15 m
L_C	Conduit length	Barclay et al. (1998)	5000 m
G	Acceleration due to gravity		10 m s^{-2}

700 m a.s.l., resulting in a dome collapse of approximately 400 m (Herd et al., 2005). This, and the estimated maximum tensile strength of the surrounding country rocks of 20 MPa provides an upper limit for the pressure change in our model (Sparks, 1997). The assumption of a magma crystallinity in equilibrium with the pressure field is not likely to be appropriate during periods of sustained magma flow due to crystallisation kinetics (Hale et al., in press). However the largest strain-rates and shear stresses are likely to be at the conduit walls due to a no-slip boundary condition. At the conduit wall, where magma is stationary, the crystal volume fraction and water content in the magma will be in equilibrium with the applied pressure. Hence the viscosity field along the conduit wall, where shear bands form, would not be expected to change much for transient flow from our unsteady model.

3.3. Temperature

The low thermal conductivity of magma means that the temperature will not change significantly along the length of the conduit, enabling us to assume the magma is in thermal equilibrium. The temperature of the magma and the conduit walls in our models is set to be 1123°K (Rutherford and Devine, 2003) justified by assuming the eruption is long-lived, the case for SHV, and therefore the conduit walls have been pre-heated. We assume that shear bands form instantaneously so that isothermal conditions prevail. Temporal offsets that may affect the flow; i.e., shear heating can further destabilize the flow once shear bands form, but this effect will be secondary to the onset of shear bands.

3.4. Physical properties of magma

Magma contains crystals, melt and bubbles that vary in proportion during flow and ascent in the conduit. Variations in the proportions of liquid and non-liquid components will modify the viscosity. The role of bubbles in the magma in the simulation is ignored because its influence upon the viscosity is weak, a maximum change in viscosity of approximately 75% (Lejeune et al., 1999) and for high viscosity dome forming eruptions this value is likely to be much lower (Pal, 2003). Our model focuses upon representing the crystal volume fraction characteristics of the magma since this has by far the strongest influence upon the magnitude of the effective viscosity, potentially increasing it to over 4 orders of magnitude (Lejeune et al., 1999; Watts et al., 2002; Melnik and Sparks, 2002; Costa, 2005). By assuming the maximum crystal volume fraction possible in the magma, our model can be considered to be an end-member scenario, reflecting very slow magma ascent rates, and will generate the deepest shear bands owing to the highest viscosity within the conduit and the highest over-pressures required to force flow.

For SHV the crystallinity in the magma chamber is calculated to be 35 to 45 vol.% phenocrysts and 15–20 vol.% microphenocrysts (Sparks et al., 2000) giving a total crystallinity between 50 and 65%. We assume an initial crystallinity of 60 vol.% at the conduit entrance (Fig. 1). The degree of crystallisation is modelled by considering the effective liquidus temperature T_{liq} which changes due to the progressive chemical change of the melt (Eq. (6)).

$$T_{\mathrm{liq}} = a_T + b_T \ln(P) + c_T \ln(P)^2 + d_T \ln(P)/P^2, \quad (6)$$

with the coefficients a_T, b_T, c_T, d_T as given by Melnik and Sparks (2005) and listed in Table 1. The equilibrium crystallinity ϕ_{eq} in the melt phase is given by (Eq. (7)):

$$\phi_{\mathrm{eq}} = \frac{A(P)\left(T - T_{\mathrm{liq}}(P)\right)}{B(P) - T}, \quad (7)$$

where $A(P)$ and $B(T)$ are functions of the pressure and are described by Melnik and Sparks (2005) and T is the temperature. The melt viscosity of the magma is calculated using an empirical equation developed by Hess and Dingwell (1996) (Eq. (8)), where the water content, the primary volatile, is $c = \alpha_s\sqrt{P}$ with α_s the solubility coefficient:

$$\log \eta_{\mathrm{m}} = -3.545 + \left(0.833 \ln c + \frac{9601 - 2368 \ln c}{T - (195.7 + 32.25 \ln c)}\right). \quad (8)$$

The total viscosity is calculated using the equation presented in Melnik and Sparks (2005) (Eq. (9)) where $\phi = \phi_{\mathrm{eq}}$:

$$\begin{aligned} \eta &= \theta(\phi)\eta_{\mathrm{m}} \\ \log(\theta(\phi)/\theta_0) &= (\arctan(\xi(\phi - \phi_0)) + \pi/2). \end{aligned} \quad (9)$$

Eq. (9) contains the coefficients θ and ξ, and ϕ_0 is the critical crystal fraction, and the values used are given in Table 1. For our model, this gives a viscosity from 5×10^5 Pa s at the magma chamber up to 4×10^{10} Pa s at the conduit exit, depending upon the magma chamber pressure used.

3.5. Magma shear strength

The shear strength provides a limit to the acceptable stress states in a material. Laboratory experiments show

that the critical stress at the onset of yield is a function of pressure, temperature, strain, strain-rate, porosity and sample size (Kearey and Vine, 1996). Therefore the physical properties of the magma are likely to affect the yield characteristics of the magma. For example, if the magma has only small amounts of crystals then the magma may yield in a ductile way as observed for metals. Whilst for cool brittle magma, deformation is localised along micro-fractures that amalgamate into a shear surface at failure (Sparks et al., 2000). Since we do not have knowledge of the yield mechanism along the conduit length we must focus on the simplest scenario, a constant magma shear strength with a magnitude obtained from the brittle-ductile criteria for glasses. For a first look into the effects of plasticity we use the von Mises visco-plastic model with the yield criterion given by Eq. (10), where F designates the yield function, $\tau = \sqrt{1/2\sigma'_{ij}\sigma'_{ij}}$ is the equivalent shear stress and τ_S is the magma shear strength. Prior to yielding the material deforms linearly (i.e. Newtonianly), and once the shear strength has been reached some fraction of the deformation will be permanent and non-reversible with plastic flow along a shear band.

$$F = \tau - \tau_S \leq 0. \tag{10}$$

For an illustration how the criterion (Eq. (10)) works, consider simple shear with a prescribed monotonically increasing strain rate. At sufficiently low strain-rates the shear stress is below the magma shear strength τ_S. As the strain rate increases the shear stress will eventually reach τ_S. It is non-physical for $\tau - \tau_S > 0$, that is to have a stress exceeding the magma shear strength, thus even if the strain rate is increased the shear stress will remain constant with $\tau = \tau_S$. Hence, shear bands are less likely to develop as the magma shear strength increases and the driving force of the process controlling the magnitude of the shear stress remains unaltered, because higher shear stresses are required to permit the magma to enter the plastic regime. To model plastic flow we define an effective viscosity $\eta_{eff} = \min[\eta, \eta_S]$ in the solution of the velocity–pressure problem (Eq. (5)), η is the pre-yield viscosity (Eq. (9)) and $\eta_S = \tau_S / \dot{\gamma}$, where $\dot{\gamma}$ is the equivalent strain-rate, i.e. $\dot{\gamma} = \sqrt{2D_{ij}D_{ij}}$. Since $\dot{\gamma}$ is unknown initially the solution has to be determined iteratively. The definition of η_{eff} ensures that after enough iterations $\tau - \tau_S \leq 0$ everywhere. Although the non-linear problem is solved iteratively using a secant rather a tangent method, the character and the properties of the solution is determined by the properties of the tangential problem (Mühlhaus and Regenauer-Lieb, 2005). During the iterations the plastic zone typically narrows and lengthens continuously until it is localised in a band of approximately one element size width along the conduit wall. In this particular case the plastic zone coincides with the domain occupied by the shear band.

Table 2 gives values for τ_S from the literature. Apparent from Table 2 is that the magma shear strength is not well constrained. Some of this scatter is because the physical properties of semi-molten magma are hard to measure given the technical difficulties involved in deforming samples of lava at the high temperatures, pressures and strain-rates that occur within natural systems.

4. Results

The axi-symmetrical Eqs. (3)–(5) are solved using the parallelized FEM based PDE solver eScript and the FE library Finley (Gross et al., 2007). More details on the solution process for the velocity and pressure fields can be found in (Hale et al., 2007). The axi-symmetric cylindrical conduit is discretised using 5000×15 elements with

Table 2
Magma shear strength values quoted in the literature for lavas that are appropriate to our study

Magma shear strength (Pa)	Reference	Comments
10^6–10^7	Romano et al. (1996)	Experimental results from hydrous vesicular glasses.
10^6	Voight et al. (1999)	From estimates for the strength of lava from the height of spines extruded at Soufrière Hills Volcano, Montserrat.
10^7	Gonnermann and Manga (2003)	Used in numerical models for magma fragmentation.
0.5–1.5×10^6	Green et al. (2006)	Inferred from numerical models for the amplitude of tilt measured at Soufrière Hills Volcano, Montserrat.
10^7	Neuberg et al. (2005)	Used in numerical models of magma flow at Soufrière Hills Volcano, Montserrat.
10^7–10^8	Tuffen et al. (2003)	Magma shear strength values from laboratory experiments.

quadratic shape functions (8 nodes/element) in conjunction with 4 point Gauss integration for the element matrices.

4.1. Shear band generation

Fig. 2 shows results from one simulation with magma shear strength of 2×10^5 Pa and a magma chamber pressure of 132.2 MPa, which required a pressure change of 14.7 MPa at the conduit exit. From left to right in Fig. 2 we produce plots of velocity in X_3-axis, strain-rate, shear stress, and shear stress divided by the magma shear strength (effectively the plasticity). Where the shear stress divided by the magma shear strength is exactly equal to unity, shear bands will form. This results in a narrow band one element wide flush against the conduit wall, and for this simulation corresponds to a shear band length of 413.5 m. In all the models presented, shear bands form a continuous band between the conduit exit and the maximum depth of the shear band directly against the conduit wall. This is due to the effective viscosity increasing towards the conduit exit (Fig. 3) and the magma shear strength having a constant value.

4.2. Shear band length

Fig. 4 shows the length that shear bands penetrate into the conduit for two different magma shear strengths over a range of magma chamber pressures, from 2.4 MPa to 25.4 MPa. Using a magma shear strength of 10^6 Pa the result was that no shear bands form in the conduit over the magma chamber pressures used. By reducing the magma shear strength we can force shear bands to form, because it effectively decreases the shear-stress required before the magma enters the plastic regime. For a magma shear strength of 5×10^5 Pa shear bands develop to a maximum depth of 130 m, whilst for a magma shear strength of 2×10^5 Pa shear bands develop to a maximum depth of 703 m. The length of the shear band within a conduit will depend upon the magma viscosity and the driving pressure. Although a magma shear strength change from 2×10^5 Pa to 5×10^5 Pa is only small, the length that shear bands form to is significantly affected because the viscosity changes occurs most dramatically in the upper conduit. Fig. 3 shows the relaxed Newtonian viscosity along the

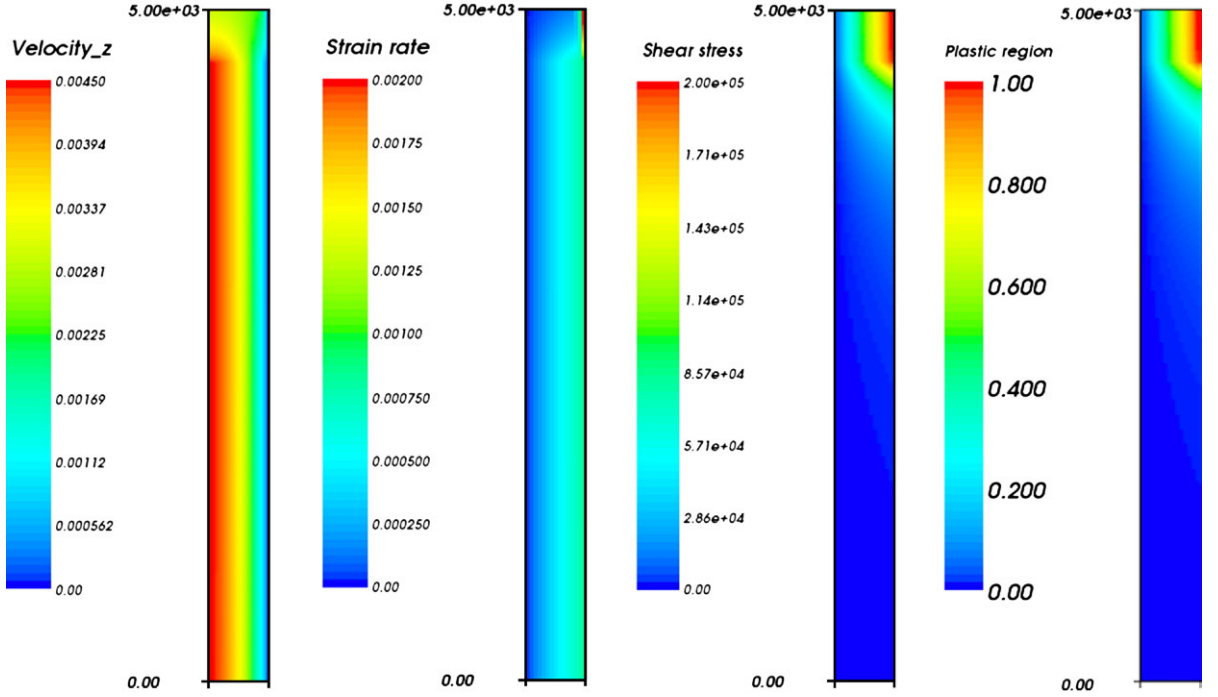

Fig. 2. Results from one simulation with a magma shear strength of 2×10^5 Pa, a magma chamber pressure of 132.2 MPa requiring a pressure change of 14.7 MPa at the free surface. From left to right are plots of velocity in the X_3-axis, strain-rate, shear stress, and shear stress divided by the magma shear strength (effectively the plasticity) within the conduit. Shown is only half of the conduit, from the centre of the conduit at $r=0$ (left side of image) to the conduit wall at $r=15$ m (right side of image). The conduit radius has been stretched in the figures by a factor of 30 to better visualise the results along the entire 5 km length of the conduit. Where the shear stress divided by the magma shear strength is exactly equal to unity shear bands develop. This corresponds to a shear band one element wide, flush against the conduit wall, within the red zone of the figure. For this simulation a shear band of length of 413.5 m forms between the conduit exit and a depth of 413.5 m.

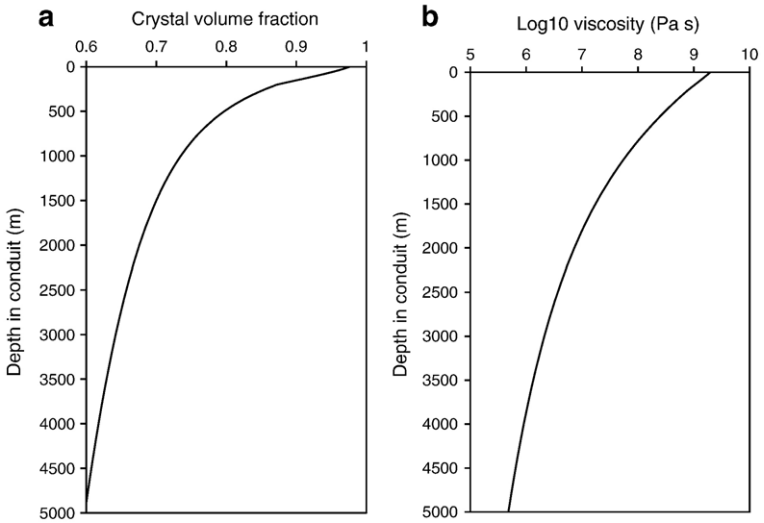

Fig. 3. A typical modelled crystal volume fraction (a) and viscosity (b) along the length of the conduit. Most of the change in viscosity and crystallinity occurs in the upper conduit due to the pressure field.

length of the conduit at the start of the simulation as well as the crystal volume fraction of the magma with depth. Fig. 4 also shows that shear bands will not form within the conduit for magma chamber pressure below approximately 130 MPa (an over-pressure of 12 MPa) for a magma shear strength of 5×10^5 Pa, whilst for a magma shear strength of 2×10^5 Pa shear bands only form for magma chamber pressures exceeding 120 MPa (i.e. an over-pressure of 2 MPa).

For low magma chamber pressures, corresponding to an initially small change in pressure at the conduit exit, the viscosity in the upper conduit will be relatively large (Eqs. (7)–(9)). However, due to the low extrusion rate (a consequence of the lower over-pressure), shear bands will not penetrate deep into the conduit. For increasing magma chamber pressures, i.e. increased dome retarding pressures, the viscosity in the upper conduit will decrease since crystallinity is a function of pressure. However, a higher over-pressure will result in a higher extrusion rate allowing the shear band length to increase with increasing magma chamber pressure. The length that shear bands penetrate into the conduit tends towards an upper limit, most clearly shown for a magma shear strength of 5×10^5 Pa (Fig. 4), due to the viscosity decreasing with increasing depth within the conduit (Fig. 3).

4.3. Shear band influence upon extrusion rate

Shear bands are likely to effect magma ascent rates by reducing conduit friction and consequently the large over-pressures required to extrude highly crystalline silicic magmas. We calculate the extrusion rate for magma flow with no shear bands in the conduit (i.e. Hagen-Poiseuille flow), assuming the magma does not enter the plastic regime. For the same magma chamber pressure we calculate the extrusion rate for magma flow in the conduit with shear bands permitted to form. Since our model ignores a possible elastic-brittle contribution to the rheology, frictional slip can not be modelled. As a consequence we model the minimum change in extrusion rate due to plastic deformation only.

Fig. 5 shows the modelled extrusion rate (a) and its relative change (b) with and without shear bands in the conduit, plotted against the pressure in the magma chamber.

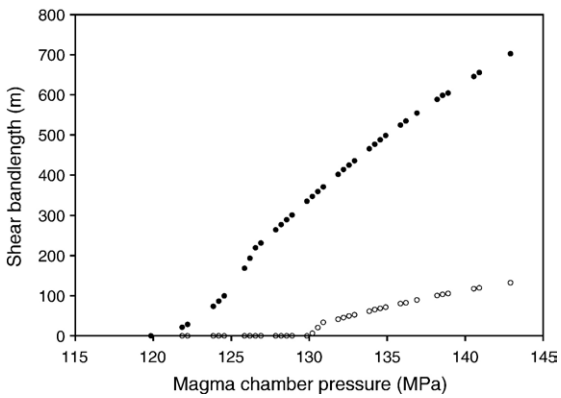

Fig. 4. Modelled shear band length against pressure in the magma chamber for magma shear strength values of 2×10^5 Pa (filled shapes) and 5×10^5 Pa (unfilled shapes). For the same magma shear strength the magma chamber pressure governs the depth of the shear bands due to its influence upon the extrusion rate and viscosity.

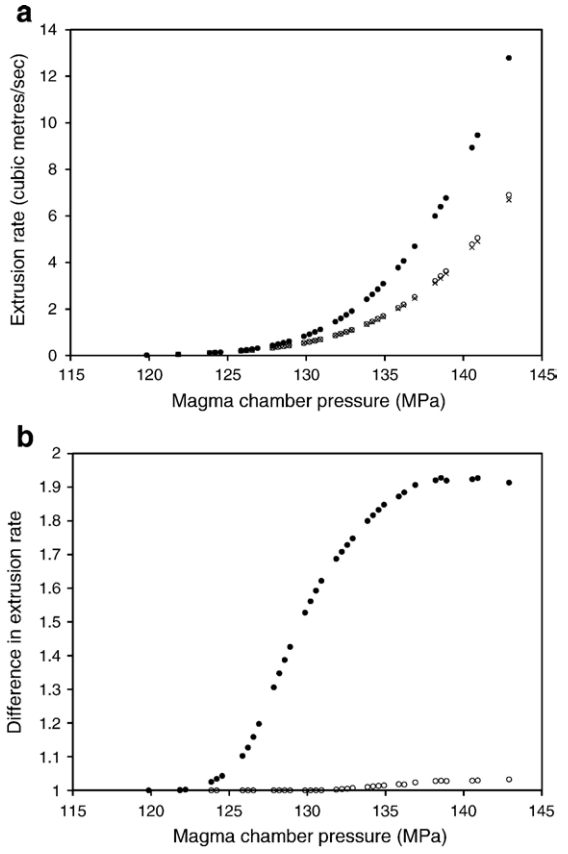

Fig. 5. Panel a shows the extrusion rate modelled with and without shear bands against the pressure in the magma chamber. The model uses a magma shear strength of 2×10^5 Pa for the solid shapes and 5×10^5 Pa for the unfilled shapes. The initial extrusion rate for no shear bands in the conduit is given by the crosses. Panel b shows the modelled change in extrusion rate (given by the extrusion rate with shear bands divided by extrusion rate without shear bands) using the same symbols for the different magma shear strengths.

For a magma shear strength of 5×10^5 Pa shear bands can penetrate to depths of 130 m, which results in a maximum change in extrusion rate of approximately 3%. Whilst for a magma shear strength of 2×10^5 Pa, at the highest magma chamber pressures shear bands reach a depth of 703 m resulting in a change in the extrusion rate of almost 100%. Transitions between effusive and explosive volcanic activity are essentially controlled by volatiles. The ability of gas trapped within the magma melt, from exsolved volatiles, to expand or escape by permeable flow will determine if the ascending magma will be effusive or explosive. Slowly ascending magma has time to release this build-up of gas resulting in highly degassed effusive magma. However, magma ascending rapidly may not be able to release the build-up of gas, and this may result in explosive activity. Gonnermann and Manga (2003) suggest that fragmentation at the conduit wall, from localised regions of high strain, may act to inhibit explosive behaviour due the enhanced permeability from the fracture network that develops. However, cyclic activity in 1997 at SHV produced numerous Vulcanian explosions with each episode preceded by a large dome collapse (Druitt et al., 2002). These collapse events may have forced the generation of shear bands in the upper conduit due to a large change in pressure as shown by our models. If these shear bands form rapidly enough, instantaneously in our visco-plastic model, the enhanced extrusion rate due to shear band formation may be large enough to prevent volatiles exsolving effusively. This may result in a competition between the processes of enhanced permeability from fragmentation and reduced gas-loss due to enhanced extrusion rates. Therefore deep shear bands may be more likely to promote explosive activity due to a potentially large increase in extrusion rate.

The relative increase in extrusion rate due to the formation of shear bands is non-linear (Fig. 5b). This is due to two processes, first the length of shear bands tends towards an upper limit due to the decrease in viscosity with depth in the upper conduit (Fig. 3). Second, at increasing depths in the conduit the viscosity is lower, which will result in a smaller decrease from Newtonian to shear viscosity, meaning that the conduit resistance change is not as significant. At low magma chamber pressures (<130 MPa) the extrusion rate is at the low end of the observed range for SHV (<0.5 $m^3 s^{-1}$). Lava is commonly extruded along shear surfaces at these extrusion rates due to the high degree of crystallinity in the magma. Since the generation of shear bands at these magma chamber pressures have a relatively minor influence upon the extrusion rate (changing it by up to 40%) this suggests that shear bands forming at this extrusion rate may be relatively stable and the crystal content will not vary significantly due to crystallisation kinetics (Melnik and Sparks, 2002).

4.4. Shear band influence upon the over-pressure field

Cyclic inflation and deflation of the flanks of the volcano as recorded by tilt-meters is indicative of pressurisation within the upper conduit (Voight et al., 1999). Crystal-rich magma forms a viscous cap in the upper conduit that inhibits flow, leading to pressure build-up at shallow levels and edifice inflation (Diller et al., 2006). The magnitude and direction of tilt of the volcano flanks can be used to infer the magnitude and depth of the pressure source. Using an isotropically pressurised model (Shepherd et al., 1998; Widiwijayanti et al., 2005) or elastic half-space model (Voight et al., 1999; Widiwijayanti et al., 2005), the depth of the pressure source is always less than 1000 m below the surface of the dome for

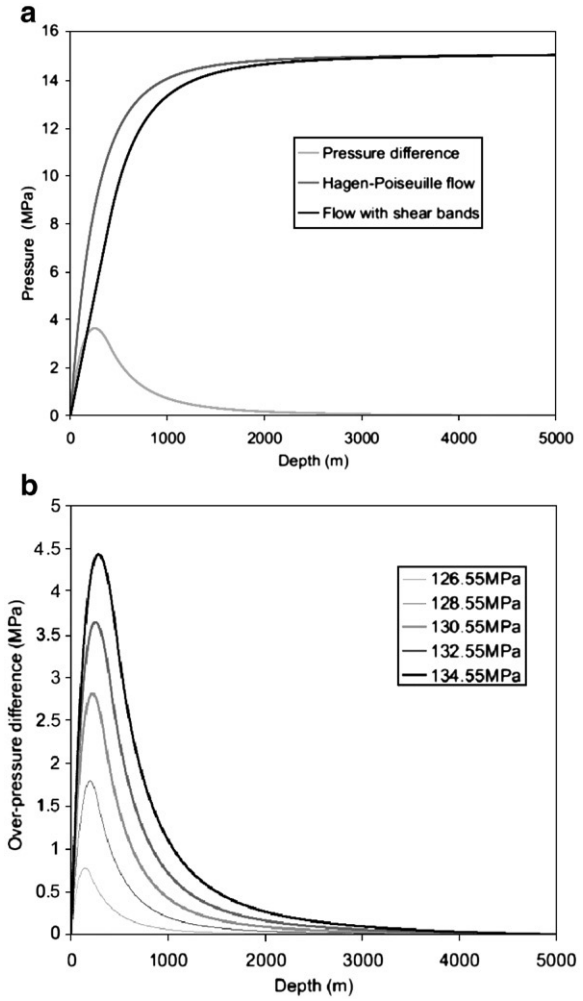

Fig. 6. (a) shows the over-pressure in the conduit with depth for flow in the conduit without shear bands (i.e. Hagen-Poiseuille flow) and with shear bands for a magma shear strength of 5×10^5 Pa (Flow with shear bands). Both flow models have a magma chamber pressure of 132.55 MPa. Also shown is the difference in pressure between the two flow regimes with depth in the conduit, a depth of zero corresponds to the conduit exit. A positive pressure difference corresponds to a decrease in the over-pressure along the conduit length, i.e. flank deflation. (b) Difference in over-pressure along the conduit due to the development of shear bands for different magma chamber pressures, shown in the legend, all for dome collapse events equivalent to 7 MPa and a magma shear strength of 5×10^5 Pa.

SHV. Also, the pressure source either needs to be very large or distributed over a large area (Widiwijayanti et al., 2005). Green and Neuberg (2006), following research by Beauducel et al. (2000), suggest that surface deformations recorded by tilt-meters could instead, or in addition, be from shear stresses within the upper conduit rather than a single large pressure source. The SHV flank displacements are then consistent with the generation of shear stresses beginning within the upper 100's metres of the conduit walls. However, Green and Neuberg (2006) emphasize that the vertical extent of the pressure source is unconstrained because tilt measurements are insensitive to deep sources. Considering vertical traction along the conduit walls the location for the tilt hypocentre is calculated to be approximately 400 m and 600 m a.s.l., that suggests a shear stress depth of 160 to 360 m below the conduit exit, with traction values between 0.5 and 1.5 MPa (Green and Neuberg, 2006). For vertical traction to explain the recorded tilt requires a pressure gradient of 6.7×10^4–2.0×10^5 Pa/m along an upper conduit segment 30 m in diameter (Green and Neuberg, 2006).

We use our conduit flow model to calculate the over-pressure within the conduit with shear bands for a magma shear strength of 2×10^5 Pa (Fig. 6). Fig. 6a shows the over-pressure profile along the conduit length for flow in the conduit with shear bands and without shear bands (i.e. Hagen-Poiseuille flow). The pressure difference in Fig. 6b corresponds to the over-pressure in the conduit for Hagen-Poiseuille flow minus the over-pressure in the conduit with shear bands for the same magma chamber pressure. Hence, what Fig. 6b shows is the redistribution in over-pressure along the conduit length due to the development of shear bands. A positive pressure difference corresponds to a drop in pressure and therefore flank deflation. Everywhere the pressure difference is less or equal (at the magma chamber and

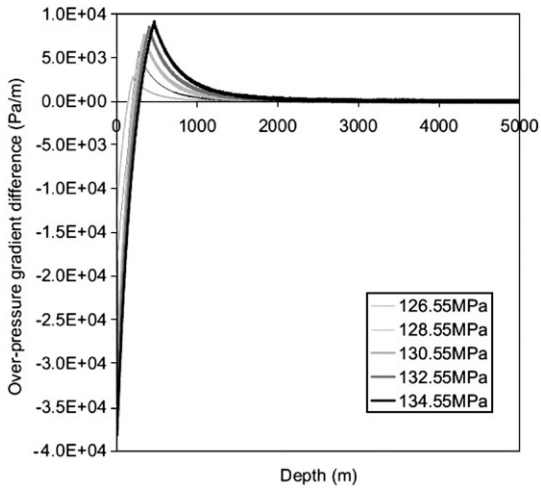

Fig. 7. Change in over-pressure gradient for flow with shear bands minus flow without shear bands (i.e. Hagen-Poiseuille flow) along the conduit length for different magma chamber pressures, shown in the legend, for dome collapse events equal to 7 MPa and a magma shear strength of 2×10^5 Pa. A positive pressure gradient corresponds to an increase in the pressure gradient due to the presence of shear bands, whilst a negative pressure gradient corresponds to a decrease. A depth of zero corresponds to the conduit exit.

conduit exit) to the initial over-pressure field, but the difference is most significant in the upper part of the conduit. This is more clearly shown in Fig. 7 which shows the over-pressure gradient along the conduit length for flow with shear bands minus that for Hagen-Poiseuille flow. Below the depth in the conduit where shear bands exist, the over-pressure gradient increases due to an increase in extrusion rate (from the presence of shear bands) but no change in viscosity. Above the depth where shear bands form, the over-pressure gradient decreases to values of 4×10^4 Pa/m. Fig. 8 shows a summary of all the model results for a magma shear strength of 2×10^5 Pa showing the pressure difference maximum and the depth of the maximum against magma chamber pressure. These values for the depth and magnitude of the pressure change are comparable to those inferred at SHV during cyclic activity.

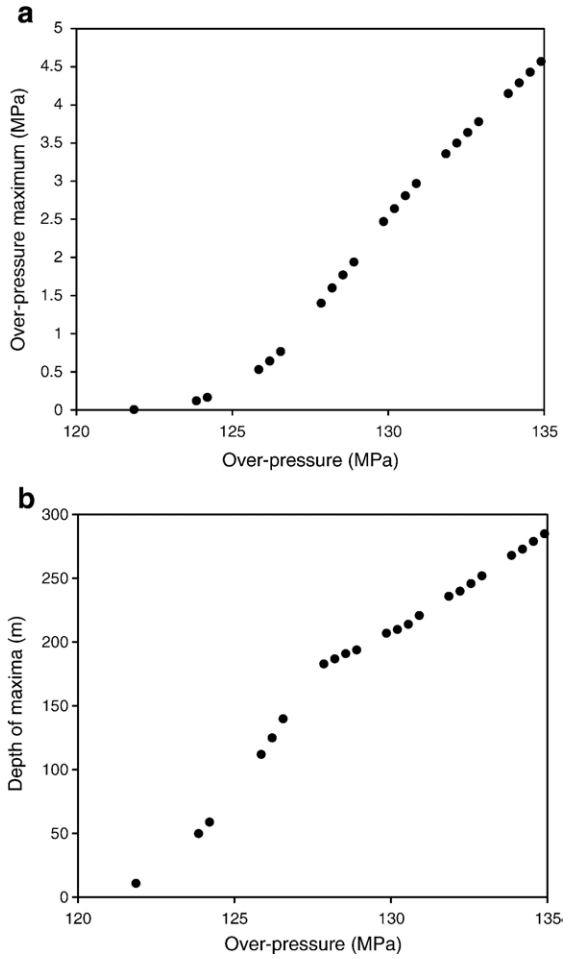

Fig. 8. Summary of a) over-pressure maximum (see Fig. 6) and b) the depth of the maxima (see Fig. 6) against magma chamber pressure for all the model runs for a magma shear strength of 2×10^5 Pa.

5. Discussion

Shear bands are simulated using a strain-localisation model to occur when the shear-stress equals the magma shear strength of the magma. This can result in the generation of shear bands to depths of approximately 700 m for low magma shear strengths (2×10^5 Pa) and high magma chamber pressures (142.9 MPa). These shear bands may be responsible for lava effusion along shear boundaries at the free surface, because they extend directly from the conduit exit, and flank inflation/deflation. Geophysical evidence for the depth of shear bands at SHV is not well constrained other than from the pressure source responsible for the inflation and deflation of the volcano flanks. Green and Neuberg (2006) and Voight et al. (1999) calculate the depth of such pressure sources to be between approximately 160 to 510 below the conduit exit, consistent with our modelled shallow shear bands depths and pressure change maximum.

The over-pressure in the upper conduit is significantly affected by the formation of shear bands, due to a change in the viscosity and flow field altering the conduit resistance. Our model shows that the over-pressure decreases in the upper conduit due to the formation of shear bands, corresponding to the deflation of the flanks. We model a change in over-pressure gradient of up to 4×10^4 Pa/m in the upper conduit and a maximum pressure change of 4.5 MPa at depths up to 300 m; magnitudes that can be related to the change in the tilt experienced during inflation and deflation cyclic events. Enhanced degassing and ash emissions are observed during the inflation maximum and deflation cycle from cracks on the dome surface (Voight et al., 1999). This may be due to the enhanced permeability from the formation of shear bands that generate micro-fractures. However there may be a competition between the process of enhanced permeability from fragmentation, and an enhanced extrusion rates suppressing gas-loss from shear band development. Also, an increase in extrusion rate due to the formation of shear bands may be the explanation for why the deflation period for the volcano flanks is commonly more rapid than the inflation period. Given further model constrains/improvements, an observed change in extrusion rate could be used to infer the shear strength of the magma within the conduit or the greatest depth that shear bands penetrate to.

The conduit of a volcano initially begins as a dyke connected to the magma chamber, with cylindrical conduit geometries only developing at shallow levels where the erosional capabilities of magma are higher. The radius or width of the dyke for SHV at depth is estimated to be approximately 11 to 12 m with an uncertainty of 7 m,

when considering the ascent rates of hornblende (Devine et al., 1998). Our model suggests that there may be a greatest depth at which upper shear bands can reach, and this will be the greatest depth at which significant conduit wall erosion will occur, when ignoring explosive decompression effects. Due to over-simplifications used in our model we can't constrain this depth. But future models that couple the change in the conduit radius with depth, and the feedback it will have upon magma viscosity and extrusion rates, will allow for an estimate of the conduit plumbing at depth.

For lower magma shear strength values the depth of shear bands can be expected to increase, but will only reach the depths at which LP seismicity occurs (~1500 m) for unrealistically low magma shear strengths. Thus, it is hard to reconcile LP seismic signals directly to the depth of shear bands simulated in our model. To form shear bands at the depth where LP events occur requires either a more complex magma shear strength model, the conduit to narrow at depth allowing the strain-rate to increase, or both. A magma shear strength model dependent upon pressure and magma crystallinity will be the focus of future research (Hale, 2007).

All models have their limitations, and we make several simplifying assumptions that are likely to affect models results. First, we have to rely upon a pressure change, via a dome collapse event, to trigger flow. However, in reality the magma is extruded without any large pressure change or dome collapse event in a continuous manner. Indeed, it was during periods of rapid magma extrusion ($>5\ m^3\ s^{-1}$) that the cyclic seismic and deformation was primarily observed. Thus a transient model including the temporal evolution of shear bands is required to fully understand the influence of shear bands upon magma flow, pressure and the timescales involved in cyclicity. Second, because we consider a maximum crystallinity in our models, this reflects flows at low extrusion rates. For flow at higher extrusion rates the viscosity is likely to be lower due to crystallisation growth kinetics (Melnik and Sparks, 1999; Hale et al., in press). This process may suppress the development of shear bands, due to a lower viscosity, resulting in lower shear stresses at the conduit wall although the crystallinity is likely to remain approximately in equilibrium at the wall. Finally, neglecting vesicularity means that we don't consider a variable density, which is likely to give quantitatively different results. Introducing vesicularity into the model will decrease the weight of the magma column which is likely to increase the extrusion rate and push the depth of shear bands to deeper levels within the conduit. However, simplifications were necessary for this model, but despite this model results suggest that changes in pressure and velocity fields due to shear bands could be significant, especially during tilt and seismic cycles in eruptive behaviour.

Acknowledgements

We would like to thank 3 anonymous reviewers for the significant changes and improvements to the manuscript and M. A. O'Brien for proof-reading. The support coming from the Australian Computational Earth Systems Simulator Major National Research Facility (ACcESS MNRF), The University of Queensland, and the ARC discovery grant DP0771377 is gratefully acknowledged.

References

Baptie, B., Luckett, R., Neuberg, J., 2002. Observations of low-frequency earthquakes and volcano tremor at Soufrière Hills Volcano, Montserrat. Mem. Geol. Soc. Lond. 21, 611–630.

Barclay, J., Rutherford, M.J., Carroll, M.R., 1998. Experimental phase equilibria constraints on pre-eruptive storage conditions of the Soufrière Hills magma. Geophys. Res. Lett. 25, 3437–3440.

Bardintzeff, J.M., McBirney, A.R., 2000. Volcanology, Second ed. Jones and Bartlett Publishers, Sudbury, Massachusetts.

Beauducel, F., Briole, P., Froger, J.L., 2000. Volcano-wide fringes in ERS synthetic aperture radar interferograms of Etna (1992–1998): deformation or tropospheric effect? J. Geophys. Res. 105, 16391–16402.

Calder, E.S., Luckett, R., Sparks, R.S.J., Voight, B., 2002. Mechanism of lava dome instability and generations of rockfalls and pyroclastic flows at Soufrière Hills Volcano, Montserrat. Mem. Geol. Soc. Lond. 21, 191–210.

Costa, A., 2005. Viscosity of high crystal content melts: dependence on solid fraction. Geophys. Res. Lett. 32, L22308.

Denlinger, R.P., Hoblitt, R.P., 1999. Cyclic behaviour of silicic volcanoes. Geology 27, 459–462.

Devine, J.D., Rutherford, M.J., Gardner, J.E., 1998. Petrologic determination of ascent rates for the 1995–1997 Soufrière Hills Volcano andesitic magma. Geophys. Res. Lett. 25, 3669–3672.

Diller, K., Clarke, A.B., Voight, B., Neri, A., 2006. Mechanisms of conduit plug formation: implications for Vulcanian explosions. Geophys. Res. Lett. 33, L20302.

Druitt, T.H., Young, S.R., Baptie, B., et al., 2002. Episodes of cyclic Vulcanian explosive activity with fountain collapse at Soufrière Hills Volcano, Montserrat. Mem. Geol. Soc. Lond. 21, 218–306.

Gonnermann, H.M., Manga, M., 2003. Explosive volcanism may not be an inevitable consequence of magma fragmentation. Nature 426, 432–435.

Green, D.N., Neuberg, J., 2006. Waveform classification of volcanic low-frequency earthquake swarms and its implication at Soufriere Hills Volcano, Montserrat. J. Volcanol. Geotherm. Res. 153, 51–63.

Green, D.N., Neuberg, J., Cayol, V., 2006. Shear stress along the conduit wall as a plausible source of tilt at Soufriere Hills volcano, Montserrat. Geophys. Res. Lett. 33, L10306.

Gross, L., Bourgouin, L., Hale, A.J., Mühlhaus, H.-B., 2007. Interface modeling in incompressible media using level sets in Escript. Phys. Earth Planet. Inter. 163 (1–4), 23–34.

Hale, A.J., 2007. Magma flow instabilities in a volcanic conduit: implications for long-period seismicity. Phys. Earth Planet. Inter. 163 (1–4), 163–178.

Hale, A.J., Bourgouin, L., Mühlhaus, H.B., 2007. Using the level set method to model endogenous lava dome growth. J. Geophys. Res. 112, B03213.

Hale, A.J., Wadge, G., Mühlhaus, H.B., in press. The influence of viscous and latent heating on crystal-rich magma flow in a conduit. Geophys. J. Int.

Herd, R.A., Edmonds, M., Bass, V.A., 2005. Catastrophic lava dome failure at Soufriere Hills Volcano, Montserrat, 12–13 July 2003. J. Volcanol. Geotherm. Res. 148, 234–252.

Hess, K.U., Dingwell, D.B., 1996. Viscosities of hydrous leucogranitic melts: a non-Arrhenian model. Am. Mineral. 81, 1297–1300.

Jaquet, O., Carniel, R., Sparks, R.S.J., et al., 2006. DEVIN: a forecasting approach using stochastic methods applied to the Soufriere Hills Volcano. J. Volcanol. Geotherm. Res. 153, 97–111.

Kearey, P., Vine, F.J., 1996. Global Tectonics, Second edition. Blackwell Science.

Kumagai, H., Chouet, B.A., 1999. The complex frequencies of long-period seismic events as probes of fluid composition beneath volcanoes. Geophys. J. Int. 138, F7–F12.

Lejeune, A.M., Bottinga, Y., Trull, T.W., Richet, P., 1999. Rheology of bubble-bearing magmas. Earth Planet. Sci. Lett. 166, 71–84.

Massol, H., Jaupart, C., Pepper, D., 2001. Ascent and decompression of viscous vesicular magma in a volcanic conduit. J. Geophys. Res. 106, 16223–16240.

Melnik, O.E., Sparks, R.S.J., 1999. Non-linear dynamics of lava dome extrusion. Nature 402, 37–41.

Melnik, O.E., Sparks, R.S.J., 2002. Dynamics of magma ascent and lava extrusion at Soufrière Hills Volcano, Montserrat. Mem. Geol. Soc. Lond. 21, 595–602.

Melnik, O.E., Sparks, R.S.J., 2005. Controls on conduit magma flow dynamics during lava dome building eruptions. J. Geophys. Res. 110. doi:10.1029/2004JB003183.

Moresi, L., Dufour, F., Mühlhaus, H.-B., 2002. Mantle convection modeling with viscoelastic/brittle lithosphere: numerical methodology and plate tectonic modeling. Pure Appl. Geophys. 159, 2335–2356.

Mühlhaus, H.-B.,, Regenauer-Lieb, K., 2005. Towards a self-consistent plate mantle model that includes elasticity: simple benchmarks and application to basic modes of convection. Geophys. J. Int. 163 (2), 788–800.

Mühlhaus, H.B., Vardoulkis, I., 1987. The thickness of shear bands in antigranular-materials. Geotechnique 37, 271–283.

Neuberg, J., Luckett, R., Baptie, B., et al., 2000. Models of tremor and low-frequency earthquake swarms on Montserrat. J. Volcanol. Geotherm. Res. 101, 83–104.

Neuberg, J.W., Tuffen, H., Collier, L., et al., 2005. The triggering mechanism of low-frequency earthquakes on Montserrat. J. Volcanol. Geotherm. Res. 153, 37–50.

Pal, R., 2003. Rheological behavior of bubble-bearing magmas. Earth Planet. Sci. Lett. 207, 165–179.

Romano, C., Mungall, J.E., Sharp, T., Dingwell, D.B., 1996. Tensile strengths of hydrous vesicular glasses: an experimental study. Am. Mineral. 81, 1148–1154.

Rutherford, M.J., Devine, J.D., 2003. Magmatic conditions and magma ascent as indicated by hornblende phase equilibria and reactions in the 1995–2002 Soufriere Hills magma. J. Petrol. 44, 1433–1454.

Shepherd, J.B., Herd, R.A., Jackson, P., et al., 1998. Ground deformation measurements at the Soufriere Hills volcano, Montserrat: II: Rapid static GPS measurements June 1996 June 1997. Geophys. Res. Lett. 25, 3413–3416.

Sparks, R.S.J., 1997. Causes and consequences of pressurisation in lava dome eruptions. Earth Planet. Sci. Lett. 150, 177–189.

Sparks, R.S.J., Young, S.R., 2002. The eruption of Soufrière Hills Volcano, Montserrat (1995–1990): overview of scientific results. Mem. Geol. Soc. Lond. 21, 45–69.

Sparks, R.S.J., Murphy, M.D., Lejeune, A.M., et al., 2000. Control on the emplacement of the andesite lava dome of the Soufriere Hills volcano, Montserrat by degassing-induced crystallization. Terra Nova 12, 14–20.

Tuffen, H., Dingwell, D.B., Pinkerton, H., 2003. Repeated fracture and healing of silicic magma generate flow banding and earthquakes? Geology 31, 1089–1092.

Voight, B., Sparks, R.S.J., Miller, A.D., et al., 1999. Magma flow instability and cyclic activity at Soufriere Hills Volcano, Montserrat, British West Indies. Science 283, 1138–1142.

Watts, R.B., Herd, R.A., Sparks, R.S.J., Young, S.R., 2002. Growth patterns and emplacement of the andesite lava dome at Soufrière Hills Volcano, Montserrat. Mem. Geol. Soc. Lond. 21, 115–152.

Widiwijayanti, C., Clarke, A.B., Elsworth, D., Voight, B., 2005. Geodetic constraints on the shallow magma system at Soufriere Hills Volcano, Montserrat. Geophys. Res. Lett. 32, L11309.

Wylie, J.J., Voight, B., Whitehead, J.A., 1999. Instability of magma flow from volatile dependent viscosity. Science 285, 1883–1885.